RESEARCH ARTICLE

Consolidation Behavior of Soft Clays with Permeability Anisotropy: A Finite Element Study

Muhammet Murat Özev[1] and Recep Akan[2,*] (ID)

[1] *Graduate School of Natural and Applied Sciences, Suleyman Demirel University, Türkiye*

[2] *Department of Civil Engineering, Faculty of Engineering and Natural Sciences, Suleyman Demirel University, Türkiye*

Abstract: The stratified nature of natural soft clay deposits fundamentally contradicts the assumption of isotropic permeability inherent in conventional consolidation theories. It assumes that the horizontal permeability coefficient (k_x) equals the vertical coefficient (k_y), although in reality, the ratio k_x / k_y can be as high as 50. A further shortcoming of the theory is that the settlements and water runoff in the soil are only assumed to occur in the vertical direction and a horizontal expansion of the soil is not possible. This study systematically elucidates the coupled effects of permeability anisotropy and model geometry on the consolidation process through 2D finite element analysis. The findings demonstrate that neglecting horizontal permeability leads to a significant overestimation of the consolidation rate and prove that the "critical width ratio" in finite element method analysis is a dynamic parameter dependent on the degree of anisotropy. Although limited to the investigated parameter range. This research provides a novel perspective on the integration of anisotropic parameters into numerical modeling for economical and safe geotechnical design. The predictive capability of the proposed regression equations encourages future investigations.

Keywords: soft clay, hydraulic anisotropy, critical width ratio, multiple regression models, finite element analysis

1. Introduction

Soil consolidation is a time-dependent process governing the long-term performance of infrastructure built on soft clay deposits. Since the pioneering work of Terzaghi [1], the theory of one-dimensional consolidation has served as the cornerstone of geotechnical design. However, the fundamental assumption of isotropic permeability ($k_x = k_y$) inherent in 1D theory is rarely met in natural sedimentary environments. Due to particle orientation during deposition and the presence of varves or seams, natural clays typically exhibit significant hydraulic anisotropy, with horizontal permeability often exceeding vertical permeability by orders of magnitude. Experimental evidence continues to verify that in natural marine clays, the horizontal permeability can exceed the vertical permeability by factors ranging from 2 to over 100, depending on the varve structure and depositional history [2, 3] as well as recent experimental findings by Gofar et al. [4].

Because anisotropic permeability governs preferential drainage directions and dissipation paths, it can materially alter seepage patterns, pore-pressure evolution, and the coupled mechanical response of soil systems; therefore, it should be incorporated into geotechnical design and analysis when directional flow is expected [5, 6]. This is particularly crucial for advanced engineering applications, as the inherent anisotropy of soft clays significantly dictates the nonlinear consolidation behavior of the surrounding soil under complex loading conditions [7].

A key limitation of Terzaghi's idealization is the assumption of vertical-only pore-water flow, whereas field conditions may involve combined vertical and lateral drainage under complex geometries. Moreover, the conventional one-dimensional consolidation framework is inherently aligned with oedometer conditions, where the specimen is confined in a rigid ring and lateral strain is restricted. In practice, boundary and friction effects in oedometer-type tests can bias interpreted stiffness/compressibility, and recent studies emphasize that ring/specimen interaction can meaningfully affect the measured response across small-to-large strain ranges [8]. Likewise, alternative consolidation devices that relax the strict 1D confinement paradigm have been discussed as a way to better approximate near-field deformation modes [9]. These points highlight that lateral deformation and non-vertical drainage are not merely theoretical nuances but can influence parameter interpretation and, ultimately, settlement prediction.

To move beyond the 1D assumptions, modern consolidation analyses commonly adopt coupled poromechanical formulations [10], in which pore-pressure dissipation and deformation of the soil skeleton are solved in a unified manner and lateral strain can be represented when needed [11–13]. Within this broader framework, recent research has developed analytical and semi-analytical solutions that explicitly address layering, anisotropy, and non-classical drainage/loading boundaries. For example, Liu et al. [14] derived an analytical solution for two-dimensional plane-strain consolidation in unsaturated soils with lateral and vertical

*Corresponding author: Recep Akan, Department of Civil Engineering, Faculty of Engineering and Natural Sciences, Suleyman Demirel University, Türkiye. Email: recepakan@sdu.edu.tr

semipermeable drainage boundaries under time-dependent loading. Similarly, Shen et al. [15] extended axisymmetric consolidation modeling for multilayered unsaturated soils by incorporating transversely isotropic permeability, demonstrating the continuing push toward more realistic geometry–hydraulic representations. In parallel, plane-strain consolidation analyses that account for anisotropic permeability have also been formulated and solved using the finite element method (FEM) [16], providing practical pathways to evaluate how k_x / k_y influences consolidation response under realistic boundary conditions.

Another widely recognized shortcoming of classical consolidation practice is the common assumption of constant soil properties during consolidation. In reality, permeability and compressibility may evolve with effective stress, strain level, and time-dependent behavior (e.g., creep). Recent developments therefore increasingly include variable/advanced constitutive descriptions and improved predictive formulations. For example, Chen et al. [17] presented a finite element model and a simplified method aimed at predicting consolidation displacement of soft soils considering creep-related aspects, reflecting the broader trend toward incorporating time-dependent behavior into settlement prediction.

Alongside analytical advances, numerical methods—particularly FEM—are now routinely used because they can represent geometry, stratification, drainage paths, and coupled hydro-mechanical response with higher fidelity than closed-form 1D solutions. Contemporary studies frequently report that, when appropriate constitutive models and parameters are used, numerical predictions can align well with field/laboratory benchmarks. For instance, combined field monitoring and 2D plane-strain FEM simulations have been used to reproduce load–settlement characteristics in improved soft ground [18]. Likewise, matching approaches for modeling prefabricated vertical drains within plane-strain finite element analyses continue to be evaluated and verified against full-scale embankment behavior [19]. Such FEM-based workflows also provide a natural platform to investigate the sensitivity of consolidation behavior to directional permeability, layer thickness, and model geometry.

Beyond settlement estimation, several recent studies demonstrate that neglecting hydraulic anisotropy can lead to underestimation of seepage pathways and potentially non-conservative stability assessments. For example, a transient seepage study on an earthen dam reported substantially increased seepage rates and reduced slope stability when anisotropic permeability was considered, compared with isotropic assumptions [20]. Similarly, reservoir slope analyses have shown that anisotropy ratio and anisotropy direction can significantly influence seepage fields, deformation patterns, and factors of safety under fluctuating hydraulic boundary conditions [2, 21, 22]. Moreover, correlations between anisotropy ratio and key soil characteristics (e.g., fines content, Atterberg limits, dry density) have been documented, supporting the view that depositional/compaction-related fabric and pore-network structure systematically contribute to hydraulic anisotropy [4]. Overall, these findings reinforce that hydraulic anisotropy can affect pore-pressure distributions and mechanical response and thus should be included in robust design-oriented modeling.

Although the influence of permeability anisotropy on seepage and slope stability has been widely investigated, its specific role in consolidation behavior—particularly in relation to numerical model geometry—remains insufficiently explored. In practical finite element analyses, horizontal and vertical permeability coefficients are still frequently assumed equal, and the selection of model width is often based on empirical judgment rather than systematic evaluation. This practice may lead to unrealistic settlement predictions and consolidation times due to boundary-induced artifacts [23]. Motivated by these limitations, the primary objective of this study is to systematically investigate the effects of hydraulic anisotropy (k_x / k_y), layer thickness (H_t), loading width (b), and model width (B) on consolidation settlement (ΔH_p) and consolidation time (t) of soft clays. Particular emphasis is placed on identifying the critical model width-to-loading width ratio required to eliminate boundary effects in finite element consolidation analyses.

In numerical geotechnical studies, particularly those focusing on parametric behavior rather than case-specific prediction, it is common practice to adopt soil parameters from experimentally validated studies and to extend them within a controlled numerical framework. The present study follows this approach by relying on material properties derived from a prior experimental–numerical investigation. To this end, a comprehensive parametric study is conducted using two-dimensional finite element modeling, and empirical correlations are developed. By explicitly addressing the combined influence of permeability anisotropy and numerical model geometry, this study aims to bridge the gap between classical consolidation theory and practical finite element modeling of soft clay deposits.

2. Consolidation

Some additional loads due to the various structures lead to increases in effective stress ($\Delta\sigma$) accompanying consolidation settlements (ΔH_t) [24]. As consolidation settlements occur gradually in saturated clays, ΔH_t must be calculated carefully before planning buildings. Figure 1 [25] illustrates the fundamental idea of the one-dimensional calculation of ΔH_t.

Figure 1
The change in the height and void ratio of clay soil samples
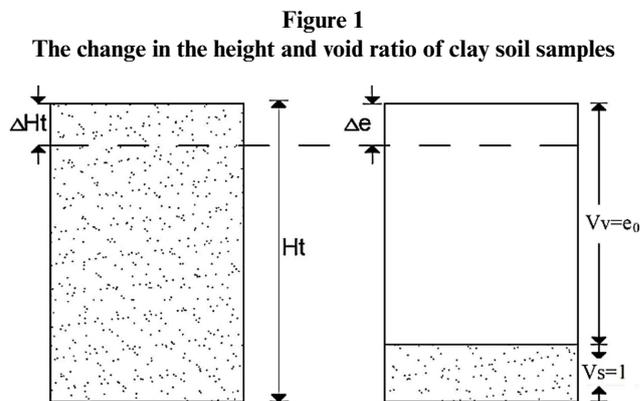
The calculation of ΔH_t for the case where the mean effective overburden pressure (σ'_0) increases to σ'_1 in a normally consolidated clay layer with a thickness similar to H_t is represented by Equation (1).

$$\Delta H_t = \frac{C_c H_t}{1 + e_0} \log \frac{\sigma'_0 + \Delta\sigma}{\sigma'_0} \tag{1}$$

where C_c and e_0 are the compression index and initial void ratio of the soil, respectively.

The rate of consolidation is influenced by the permeability of the soil and the distance water must travel before it reaches the free drainage area. It should be estimated how quickly the final settlements will occur under the planned structures [26].

The following equation can help determine how long it will take for the consolidation settlement to be completed.

$$t = \frac{T_v H_d^2}{c_v} \tag{2}$$

where t, T_v, H_d, and c_v are the time of consolidation, dimensionless time factor, length of the drain path, and consolidation coefficient, respectively.

3. Materials and Methods

3.1. Finite element method (FEM)

FEM is a method that utilizes differential equations to decompose a complex geometry problem into smaller components connected by nodes and is employed by numerous programs to solve problems [27]. In this method, many material properties, such as the contribution of elastic and plastic deformation, yield surfaces, and strength properties of the soil, determine the actual behavior of the soil [27]. Plaxis 2D v20, a computer program based on finite elements, is used to perform FEM analyses in this study. Plaxis 2D employs the FEM formulation derived from Biot's unified consolidation theory for consolidation analysis [10]. Additionally, Darcy's law is applied to the behavior of fluid, while the plane-strain model is used in the analysis. The study investigates the consolidation behavior of soft clay under a uniform load of 50 kPa applied to a foundation represented by a plate element. The models have various parameters including H_t, B, and b values, as well as different horizontal permeability coefficient values for the clayey soil.

3.2. Materials

There are numerous soil models available in Plaxis 2D v20, including the Mohr–Coulomb, Hardening Soil, Modified Cam Clay, and Soft Soil Models. The Soft Soil Model (SSM) is employed because it effectively simulates the compressive behavior of very soft soils, assuming a logarithmic relationship between volumetric strain and average effective stress [28]. Furthermore, Uysal et al. [29] showed that the laboratory test results and the numerical analysis results align with the SSM (Figure 2) [29]. Therefore, the soil parameters of soft clay used in the current study, which are inspired by Uysal et al. [29], are listed in Table 1 [29], and the material properties of the foundation are listed in Table 2.

Table 1
**Summary of material properties of the soft soil used in the finite element models**

Parameters	Symbol	Unit	Values
Unsaturated unit weight	γ_{unsat}	kN/m^3	16.50
Saturated unit weight	γ_{sat}	kN/m^3	17.30
Modified compression index	λ^*	–	0.04
Modified swell index	κ^*	–	4E-3
Cohesion	c'_{ref}	kN/m^2	30
Internal friction angle	ϕ'	°	35
Horizontal permeability	k_x	m/day	0.03E-3 0.06E-3 0.09E-3 0.30E-3
Vertical permeability	k_y	m/day	0.03E-3
Lateral earth pressure coefficient	K_0^{nc}	–	0.4264
Slope of the critical state line	M	–	1.872

Table 2
Summary of material properties of the foundation used in the finite element models

	Symbol	Unit	
Material type	–	–	Elastic
Unit weight	w	kN/m/m	0
Axial stiffness	EA1	kN/m	23.5E6
Bending stiffness	EI	kN m^2/m	1.65E6
Poisson ratio	ν	–	0.15

The soil parameters adopted in this study were not arbitrarily selected. Instead, they were obtained from a previously published experimental study [29] in which comprehensive laboratory tests were conducted on soft clay specimens, and the measured

Figure 2
Determination of (a) modified compression index and (b) swelling index values, confirming the experimental results for the 150–200 kPa loading stage
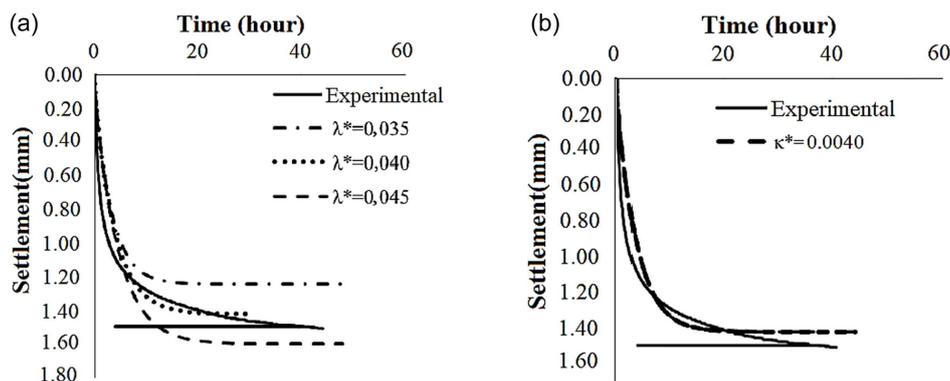
consolidation behavior was subsequently reproduced through finite element modeling. By adopting these validated material parameters and preserving the original constitutive framework, the present study builds upon an experimentally supported numerical basis. The primary objective of the current work is therefore not experimental reproduction, but a systematic parametric investigation focusing on the effects of hydraulic anisotropy and model geometry within a consistent and literature-supported numerical framework.

3.3. Model validation

The investigations indicated that the settlement amount was approximately 1.5 mm, and the consolidation time was roughly 170 days due to loads on an area 80 cm broad. Figure 2 [29] indicates that the settlement amount aligns closely with the experimental result. The experimental specimen has a thickness of 15 cm, while the effective depth in the FEM model is 160 cm, assumed to be twice the loading area. The consolidation time remains consistent, and the approach positing that the rate of consolidation correlates with the square of the layer thickness is considered.

3.4. Model geometry and boundary conditions

The models allow vertical deformation at the vertical boundaries but restrict horizontal displacement. Deformation is prohibited in both directions at the lower boundary but allowed in all directions at the upper boundary. The soil is fully saturated, and water drainage is permitted at all boundaries. Analysis of consolidation settlement and consolidation times at medium, fine, and very fine mesh levels revealed settlements of 1566 mm, 1538 mm, and 1675 mm, and consolidation times of 144.8 days, 142.2 days, and 170.2 days, respectively (Table 3). Therefore, to maintain the accuracy of the results, "very fine" mesh was applied to the perimeter of the base, and "medium" mesh was applied to remain of the model to keep the analysis time efficient. The mesh consists of 15-node triangular elements. Figure 3 shows the model geometry, finite element mesh, boundary conditions, and Point A, which is located at the center of the foundation where ΔH_t is measured.

In this study, the effects of H_t, B, b, and k_R on the consolidation behavior of soft clays are investigated. Soft clay layers with various thicknesses and horizontal permeability coefficients are loaded along various widths. Additionally, different model widths are examined by doubling each model's width, starting from the load width. A total of 520 different models are solved within the range of corresponding parameters specified in Table 4.

Table 3
The consolidation settlements and time vary with the mesh size in the FEM models

	Mesh	Thickness cm	Settlements mm	Time days
	Medium		1.566	144.8
FEM mode	Fine	15	1.538	142.2
	Very fine		1.675	1702
Experimental	–	160	1.5	1.5

Figure 3
Mesh and boundary conditions of the FEM model
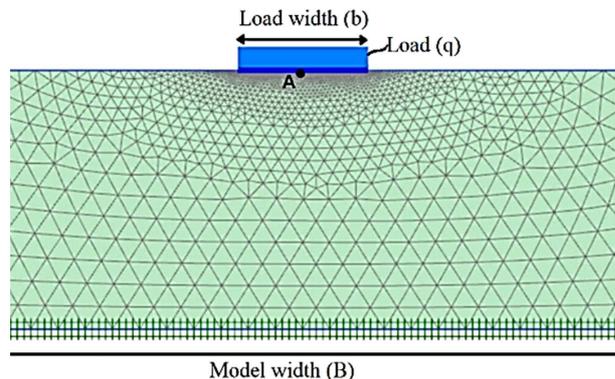
Table 4
The range of parameters considered in parametric studies

Variables	Symbol	Unit	Values
Layer thickness	H_t	m	2, 5, 10, 50
Hydraulic anisotropy ratio	k_R		1, 2, 3, 10
Loading width	b	m	0.5, 2, 4
Model width/loading width	B / b		1, 2, 4, 8, 16, 32, 64, 128, 256, 512, 1024, 2048, 4096

4. Results and Discussion

This section presents the results of the finite element analyses, focusing on the variation of consolidation settlement and time under various permeability anisotropy ratios and model geometries for layers with different thicknesses.

4.1. Effect of model geometry on consolidation settlement and consolidation time

Figure 4 shows the change in ΔH_t as a function of B / b for b values of 0.5 m, 2 m, and 4 m, where $k_R = 1$ and $H_t = 10\ m$. ΔH_t increases by 2.79 and 4.29 times when b is increased by 4 and 8 times, respectively. ΔH_t increases with increasing b values because the effective depth increases. Critical width ratio (CWR) is 32, 12, and 10 for b values of 0.5 m, 2 m, and 4 m, respectively. The trends observed in the settlement results clearly demonstrate the influence of numerical boundary conditions on consolidation behavior. The sharp increase in settlement observed at low B values highlights the sensitivity of consolidation response to lateral boundary constraints. Narrow models exaggerate settlement predictions by preventing natural horizontal expansion, whereas models exceeding the CWR accurately represent field-like deformation conditions. As the model width increases beyond the CWR, the stress redistribution becomes insensitive to boundary effects, leading to convergent and physically realistic settlement values.

Figure 5 shows how t varies with B / b for the models with b values of 0.5 m, 2 m, and 4 m, where $H_t = 10\ m$. t increases by

Figure 4
The variation of consolidation settlement versus the model geometry for various foundation widths
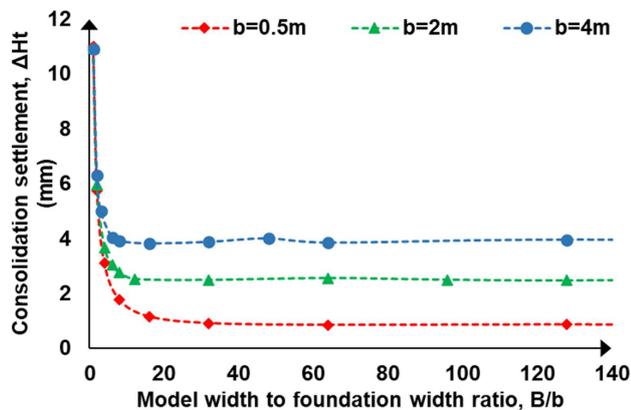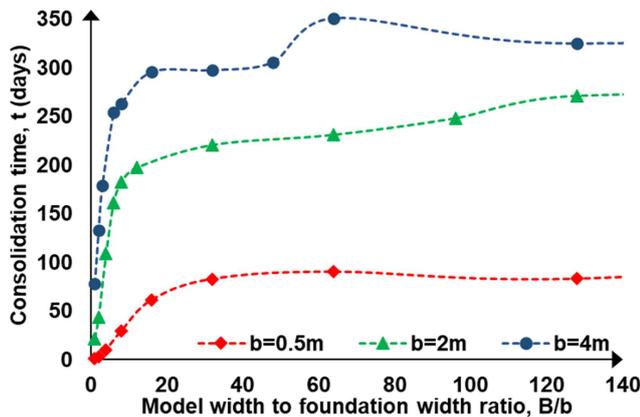

Figure 5
The change in total consolidation time while the width of the FEM model increases for different foundation widths

factors of 2.44 and 3.27 when b is increased by factors of 4 and 8, due to the increase in adequate depth, respectively.

The results further reveal that the benefit of anisotropy is sensitive to the loading geometry. For narrow loading widths, the horizontal drainage effect is pronounced. Conversely, for wide loading areas, the behavior approaches the 1D condition regardless of the horizontal permeability coefficient.

4.2. Effect of permeability anisotropy on consolidation settlement

The variation of ΔH_t as a function of B/b for the models with 2 m, 5 m, 10 m, and 50 m of H_t and $b = 0.5\,m$ for different k_R values is shown in Figure 6. ΔH_t reaches very high values when $B \approx b$. At the same time, it gradually decreases with increasing B and then remains constant for sufficiently large values of B. The reason why the settlement values change with B is that the vertical model boundaries prevent lateral deformation; however, after a certain point, the lateral effect does not reach the model boundaries. CWR values are 14 and 12 for $H_t = 2\,m$, while $k_R = 1$ and $k_R = 10$, respectively. CWR values are 48 and 30 for $H_t = 10\,m$, while $k_R = 1$ and $k_R = 10$, respectively.

ΔH_t increases by 2.3, 4, and 11.38 times when $B \approx b$ and by 1.25, 1.33, and 1.5 times when $B = CWR$, while H_t increases by 2.5, 5, and 25 times, respectively. ΔH_t may be overestimated,

especially when the compressible layer is thick, particularly when $B \approx b$, because the decrease in effective stress through depth cannot be adequately reproduced due to the model boundary conditions for models with width ratios smaller than CWR.

Figure 7 shows the change in ΔH_t versus B/b for k_R values of 1, 2, 3, and 10, with $b = 0.5\,m$. It is seen that k_R does not influence ΔH_t. The results indicate that hydraulic anisotropy has a negligible effect on consolidation settlement magnitude. This behavior suggests that settlement is primarily governed by soil compressibility and effective stress distribution, whereas permeability anisotropy mainly controls the rate of pore-pressure dissipation rather than the final deformation level.

4.3. Effect of permeability anisotropy on consolidation time

Figure 8 illustrates the variations in t versus B/b for the models with H_t values of 2 m, 5 m, 10 m, and 50 m, where $b = 0.5\,m$. There is a consistent B value for evaluating t and ΔH_t as more realistic. t values are close to each other and unrealistic for models, whereas $B \approx b$ due to the rapid discharge of water in the horizontal direction. The t increases with increasing B, while it remains constant for models, whereas B/b is greater than CWR.

Figure 9 shows the change in t versus k_R, where H_t values are 2 m, 5 m, and 10 m, and $b = 0.5\,m$. The t value decreases nonlinearly with increasing k_R, particularly for small H_t values. Also, t increases by factors of 3.92, 7.90, and 11.63, while H_t increases by factors of 2.5, 5, and 25 with $k_R = 1$, respectively. In addition, t increases by factors of 3.2 and 5.40 when H_t increases by factors of 2.5 and 5, respectively, while for $k_R = 10$. The influence of H_t on t becomes more apparent with a decrease in k_R. Also, as clearly observed, the curves exhibit a downward trend as the anisotropy ratio increases from 1 to 10. This trend quantitatively shows that lateral drainage significantly shortens the drainage path, a phenomenon that is disregarded in isotropic models. For instance, for $H_t = 10\,m$, the consolidation time in the isotropic case ($k_R = 1$) is approximately 150% higher than the anisotropic case ($k_R = 10$).

Figure 10 illustrates the change in t as a function of B/b, where k_R values are 1, 2, 3, and 10, and $b = 0.5\,m$. t increases by 0.86, 0.80, and 0.63 times for $H_t = 2\,m$ and by 0.73, 0.62, and 0.42 times for $H_t = 10\,m$, while k_R values increase by 1, 2, 3, and 10 times, respectively. t is influenced by k_R in contrast to ΔH_t, so that horizontal permeability affects the consolidation time but not the consolidation settlement significantly. CWR values are 16 and 56, whereas $H_t = 2\,m$ and $H_t = 10\,m$, respectively, while $k_R = 10$. According to the literature, CWR should be greater than 5 for stability analysis, while it is 7 and 9 for drained deformation analysis and undrained deformation analysis, respectively, for embankments [28]. The results of the current study generally led to larger CWR values than the corresponding recommendations. In addition, previous research generally does not consider the effects of H_t and k_R on determining CWR. However, the present study demonstrates that H_t and k_R have a significant impact on CWR. The influence of hydraulic anisotropy on consolidation time becomes more pronounced as the layer thickness increases. In thick layers, lateral drainage paths dominate the dissipation process, making consolidation time increasingly dependent on horizontal permeability.

Recall that the primary objective of this study was to quantify the error margin introduced by the isotropic permeability assumption. Our results directly address this by demonstrating that neglecting anisotropy leads to an overestimation of

Figure 6
Variation of consolidation settlement according to model geometry for various layer thicknesses while (a) $k_R = 1$ and (b) $k_R = 10$
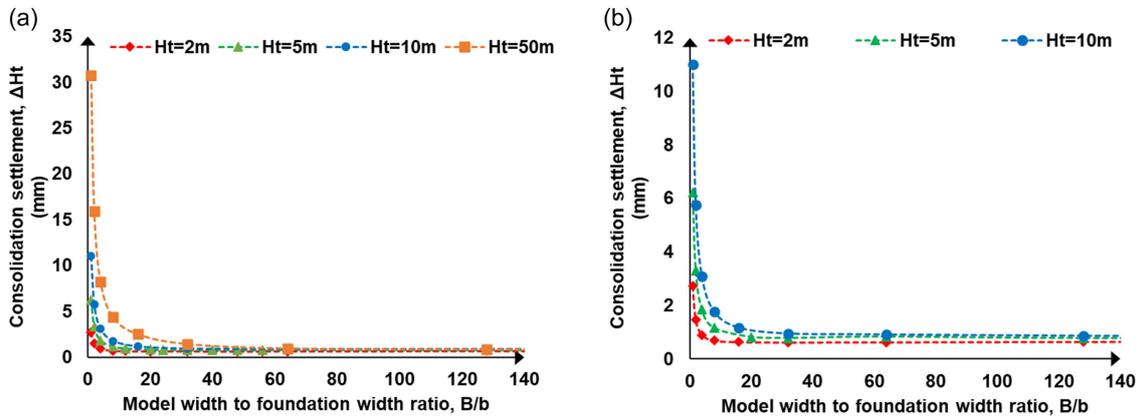

Figure 7
The variation of consolidation settlement versus the model geometry at different permeability anisotropy ratios for (a) $H_t = 2\ m$ and (b) $H_t = 10\ m$
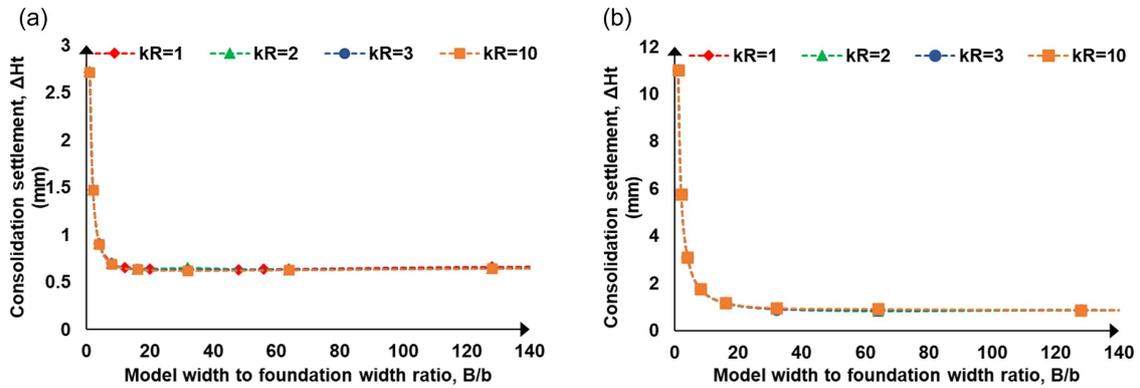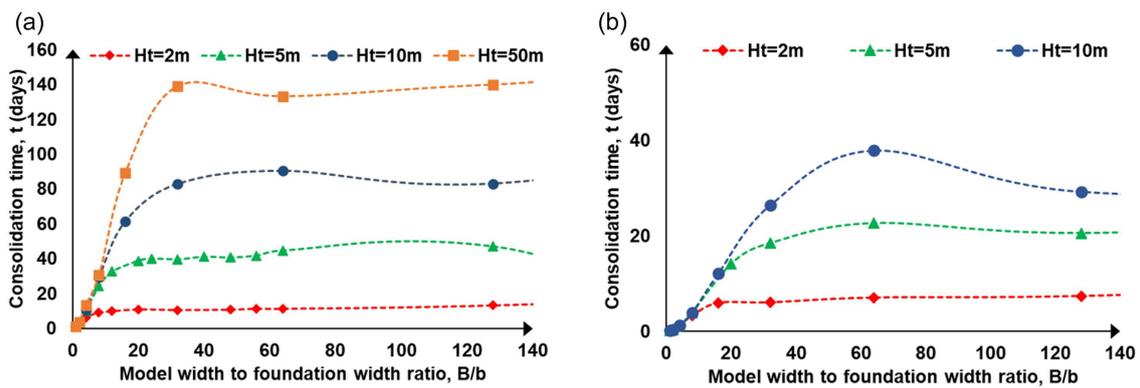

Figure 8
The variation of total consolidation time as a function of the model geometry for different layer thicknesses, whereas (a) $k_R = 1$ and (b) $k_R = 10$

consolidation rates by up to 150%. This explicitly confirms the study's hypothesis that 1D conventional theories are insufficient for accurately predicting settlement times in stratified soft clays.

When Figure 10(c) is examined in particular, comparing the values on the flat part of the curves, it is seen that the consolidation time is 29.24, 53.09, 68.54, and 83.2 when the anisotropy ratio is 1, 2, 3, and 10. This shows that, according to the isotropic assumption, the consolidation time increases by 81%, 29%, and 21%, respectively, due to the effect of anisotropy. The numeri-

cal analyses clearly demonstrate that the rate of consolidation is governed not only by the drainage path length but also significantly by the permeability ratio. From a theoretical standpoint, this acceleration is attributed to the activation of preferential horizontal drainage paths. In the isotropic case, pore water follows the longest path vertically toward the drainage boundary. However, as horizontal permeability increases, the hydraulic gradient drives water laterally toward the free field, effectively shortening the drainage path. This contradicts the conventional assumption

Figure 9
The change in total consolidation time while the anisotropy ratio increases for different layer thicknesses
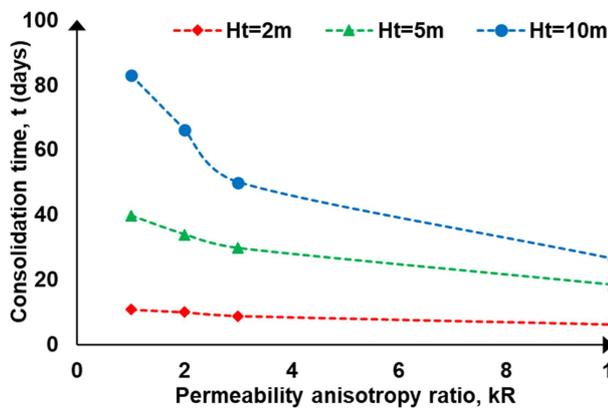
that settlement is solely controlled by vertical flow, a limitation also highlighted by Shen et al. [15] in analytical solutions for multilayered systems.

Furthermore, the existence of a critical model width-to-loading width ratio observed in this study is consistent with numerical modeling practices reported in previous FEM-based consolidation and embankment analyses. Similar recommendations regarding minimum model width requirements to eliminate boundary effects have been reported in numerical studies and software guidelines [28]. The present findings further extend these observations by demonstrating that the CWR is not constant but influenced by soil layer thickness and permeability anisotropy.

Previous analytical and numerical studies have demonstrated that permeability anisotropy has a limited influence on consoli-

dation settlement but significantly affects consolidation time by altering drainage efficiency and pore-pressure dissipation paths [11, 14, 16]. The observed acceleration of consolidation with increasing horizontal permeability ratio in this study is therefore in good agreement with established theoretical expectations and prior FEM-based investigations.

4.4. Multiple regression analysis results

In this section study, regression analyses are performed to estimate ΔH_t and t using FEM results from models exceeding the CWR. ΔH_t curves versus H_t are plotted for $b = 0.5\ m$ and $b = 2\ m$, where $q = 50\ kPa$ and $k_R = 1$ in Figure 11. The suitability of the regression models was verified through R^2 values to ensure statistical validity. There is a logarithmic relationship between H_t and ΔH_t for $b = 0.5\ m$ but not for $b = 2\ m$. However, it is considered a logarithmic function in Figure 11(b), though it shows a linear relationship to obtain a generalized function that covers both cases. A generalized logarithmic function was adopted to maintain consistency across different layer thicknesses. Although the high R^2 values indicate strong internal consistency, extrapolation beyond the investigated parameter ranges should be approached with caution.

A generalized logarithmic equation that covers the case for both $b = 0.5\ m$ and $b = 2\ m$ is created by combining the correlations of the curves from Figure 11(a) and 11(b). Equation (3) estimates the consolidation settlement according to b and H_t in the range of the study. It assumes that b, H_t, and ΔH_t are given in cm, m, and mm, respectively.

$$\Delta H_t = (0.0032b - 0.0513)\ln(H_t) + 0.0041b + 0.3884 \tag{3}$$

Figure 10
Variation of *t* versus *B/b* for different k_R values, whereas (a) $H_t = 2\ m$, (b) $H_t = 5\ m$ and (c) $H_t = 10\ m$
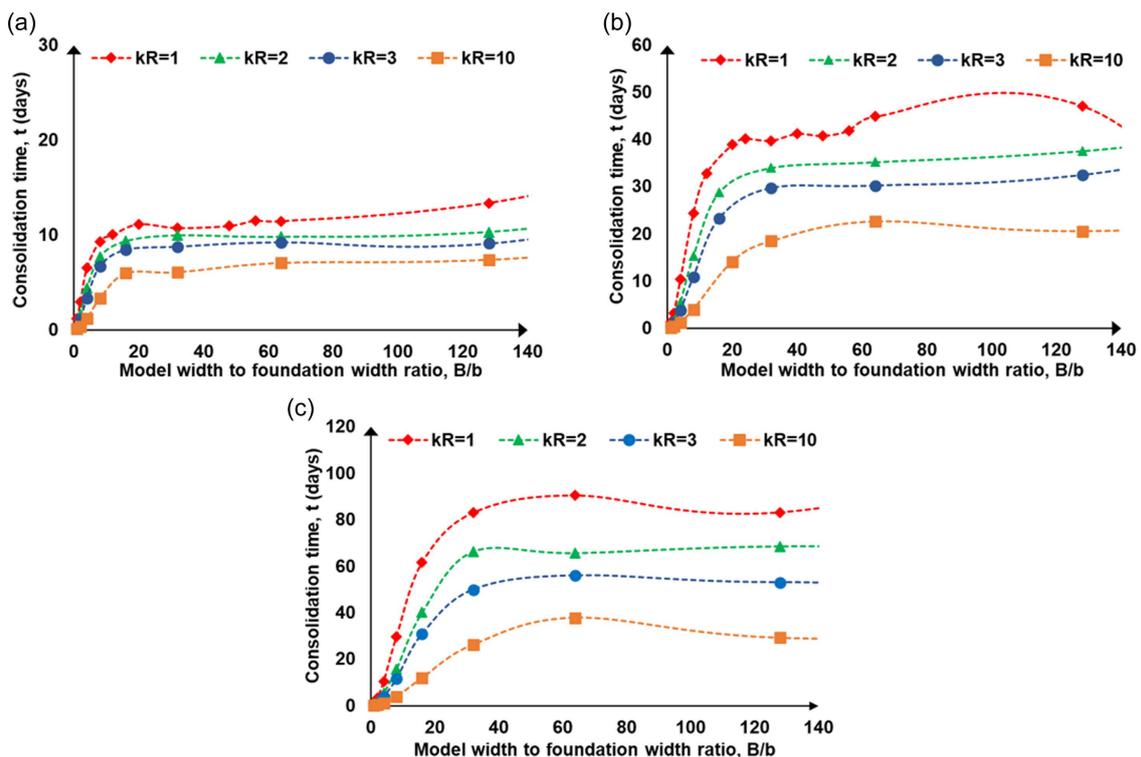
Figure 11
ΔH_t **versus** H_t **for (a)** $b = 0.5\ m$ **and (b)** $b = 2\ m$
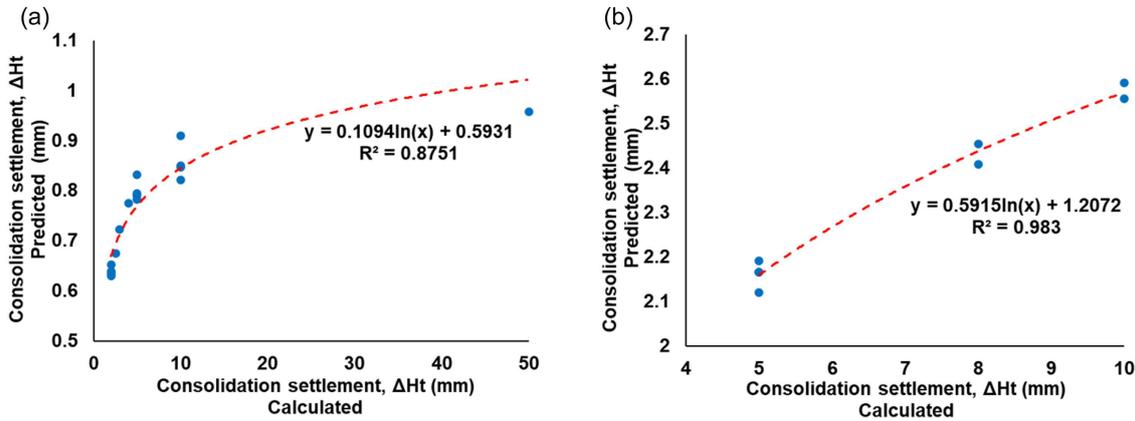
Figure 12
Scatter plots of ΔH_t **values predicted by Equation (3) and calculated by FEM analysis**
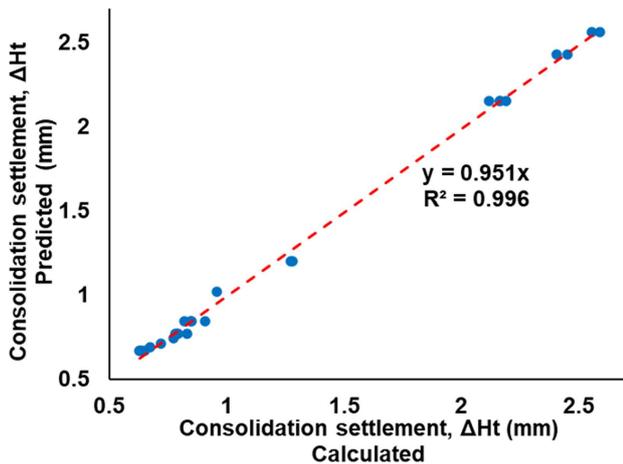
Figure 13
t **as a function of** k_R **for different** H_t **values**
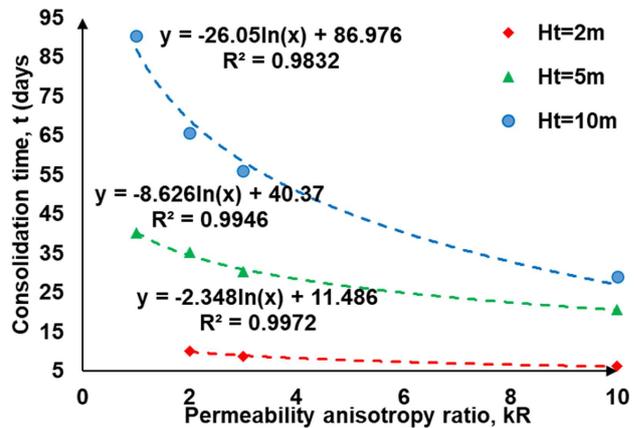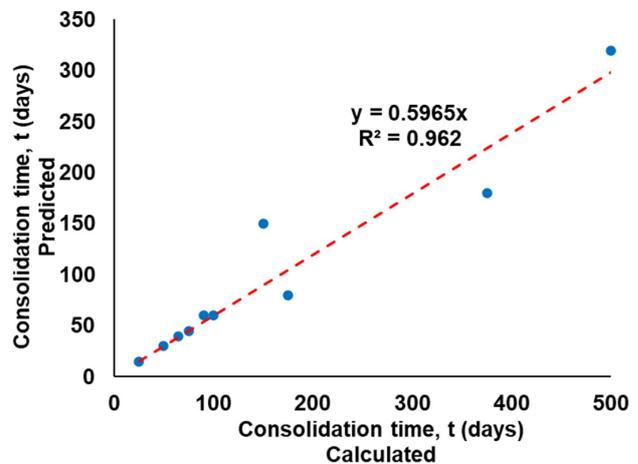

Figure 14
Scatter plots of ΔH_t **values predicted by Equation (4) and calculated by FEM analysis**

The ΔH_t values obtained from FEM analysis and the ones predicted by Equation (3) are plotted in Figure 12 to evaluate compatibility. R^2 is determined to be 0.99, indicating that Equation (3) demonstrates strong predictive performance within the investigated parameter ranges. Although the proposed empirical correlations are primarily valid within the investigated parameter ranges, the results are highly promising for practical engineering applications. By enabling rapid estimation of consolidation settlement and time under anisotropic conditions, these models offer significant time savings and practical benefits during the preliminary design phase of geotechnical projects. Furthermore, the strong internal consistency and high predictive accuracy observed in this study provide a robust foundation that encourages future expanded research.

Figure 13 shows the variations of t as a function of k_R for the models with H_t values of 2 m, 5 m, and 10 m, where $B = CWR$, $b = 0.5\ m$, and q = 50 kPa. t and k_R are logarithmically related, as shown in Figure 13. To address the situations when H_t values are 2 m, 5 m, and 10 m, the pertinent logarithmic relations are merged and converted into Equation (4). H_t and t are assumed to be provided in m and days, respectively, in Equation (4).

$$t = -0.8189 H_t^{1.843} \ln k_R + 9.4245 H_t - 7.1282 \tag{4}$$

To assess the agreement between t-values calculated by the FEM analysis and those predicted using Equation (4), the results are plotted in Figure 14. It is evident that Equation (4) demonstrates strong predictive performance within the investigated parameter ranges, with an R^2 value of 0.96.

5. Conclusion

This study investigated the consolidation behavior of soft clays through a parametric two-dimensional finite element analysis, explicitly accounting for hydraulic anisotropy and numerical model geometry. The following main conclusions were obtained:

1) Hydraulic anisotropy was found to have a negligible influence on the magnitude of consolidation settlement; however, it plays a dominant role in controlling consolidation time by governing drainage efficiency and pore-pressure dissipation paths.
2) The commonly adopted assumption of isotropic permeability may lead to systematic deviations in consolidation behavior, leading to significant deviations in predicted consolidation time.
3) Isotropic permeability assumptions were shown to systematically overestimate consolidation rates, with consolidation time being overpredicted by up to approximately 150% compared to anisotropic conditions.
4) Overall, the findings highlight that neglecting horizontal drainage paths constitutes a significant modeling simplification that may lead to misleading predictions. The routine incorporation of hydraulic anisotropy into numerical consolidation analyses is therefore recommended to ensure more accurate, economical, and reliable geotechnical designs.
5) A critical width-to-loading width ratio (CWR) was identified, beyond which numerical boundary effects on settlement and consolidation time become insignificant; this ratio was shown to depend on soil layer thickness and permeability anisotropy rather than being a constant geometric parameter.
6) Although limited to the investigated parameter range, the proposed regression equations exhibit encouraging predictive capability and demonstrate potential for efficient preliminary design applications.

A limitation of the present study is the absence of direct experimental or analytical verification. However, this study is intentionally designed as a parametric numerical investigation based on experimentally supported material properties adopted from the literature. Furthermore, all results obtained are limited to the scope of the study, and future experimental or analytical studies are recommended to further benchmark the proposed correlations under different soil conditions.

Ethical Statement

This study does not contain any studies with human or animal subjects performed by any of the authors.

Conflicts of Interest

The authors declare that they have no conflicts of interest to this work.

Data Availability Statement

Data sharing is not applicable to this article as no new data were created or analyzed in this study.

Author Contribution Statement

Muhammet Murat Özev: Conceptualization, Methodology, Software, Validation, Formal analysis, Investigation, Resources, Data curation, Writing – original draft, Writing – review & editing, Visualization. **Recep Akan:** Conceptualization, Methodology, Validation, Writing – review & editing, Supervision, Project administration.

References

[1] Terzaghi, K. (1925). Principles of soil mechanics: III. Determination of permeability of clay. *Engineering News Record*, *95*(21), 832–836.

[2] Yu, S., Ren, X., Zhang, J., Wang, H., & Zhang, Z. (2020). Sensibility analysis of the hydraulic conductivity anisotropy on seepage and stability of sandy and clayey slope. *Water*, *12*(1), 277. https://doi.org/10.3390/w12010277

[3] Dong, J. J., Tu, C. H., Lee, W. R., & Jheng, Y. J. (2012). Effects of hydraulic conductivity/strength anisotropy on the stability of stratified, poorly cemented rock slopes. *Computers and Geotechnics*, *40*, 147–159. https://doi.org/10.1016/j.compgeo.2011.11.001

[4] Gofar, N., Satyanaga, A., Aventian, G. D., Pernebekova, G., Argimbayeva, Z., Moon, S. W., & Kim, J. (2024). Factors affecting hydraulic anisotropy of soil. *Geomechanics and Engineering*, *36*(4), 343–353. https://doi.org/10.12989/gae.2024.36.4.343

[5] Yao, M., Wang, H., Yu, Q., Li, H., Xia, W., Wang, Q., . . . , & Lin, J. (2023). Anisotropy study on the process of soil permeability and consolidation in reclamation areas: A case study of Chongming East Shoal in Shanghai. *Buildings*, *13*(12), 3059. https://doi.org/10.3390/buildings13123059

[6] Ng, C. W. W., Qu, C., Ni, J., & Guo, H. (2022). Three-dimensional reliability analysis of unsaturated soil slope considering permeability rotated anisotropy random fields. *Computers and Geotechnics*, *151*, 104944. https://doi.org/10.1016/j.compgeo.2022.104944

[7] Shi, J., Li, X., Guo, R., Li, D., Gong, S., & Ling, D. (2026). Effect of anisotropic behavior of soft clay on the nonlinear consolidation of composite pile-improved soft ground considering size and rotational hardening. *International Journal for Numerical and Analytical Methods in Geomechanics*, *50*(3), 1572–1590. https://doi.org/10.1002/nag.70181

[8] Yoo, Y., Lee, J.-S., Han, W., & Park, J. (2025). A comprehensive consideration of friction effect on small-to-large strain stiffness: Floating versus fixed-ring oedometer cells. *Geomechanics and Geophysics for Geo-Energy and Geo-Resources*, *11*(1), 99. https://doi.org/10.1007/s40948-025-01029-y

[9] Owusu-Yeboah, Z., Sun, J., & Chen, C. (2025). Innovations in one-dimensional consolidation: A review of the double-action oedometer. *European Journal of Materials Science and Engineering*, *10*(2), 95–108.

[10] Biot, M. A. (1941). General theory of three-dimensional consolidation. *Journal of Applied Physics*, *12*(2), 155–164. https://doi.org/10.1063/1.1712886

[11] Schiffman, R. L. (1958). Consolidation of soil under time-dependent loading and varying permeability. *Proceedings Highway Research Board*, *37*, 584–617.

[12] Zhuang, Y. C., Xie, K., & Li, X. (2005). Nonlinear analysis of consolidation with variable compressibility and permeability. *Journal of Zhejiang University Science*, *6*(3), 181–187. https://doi.org/10.1631/BF02872317

[13] Wong, L. S., & Somanathan, S. (2019). Analytical and numerical modelling of one-dimensional consolidation of stabilized peat. *Civil Engineering Journal*, *5*(2), 319–412. https://doi.org/10.28991/CEJ-2019-03091254

[14] Liu, Y., Zheng, J.-J., You, L., Lu, J.-T., Cui, L., Yang, W.-Y., & Huang, Z.-F. (2022). An analytical solution for 2D plane strain consolidation in unsaturated soils with lateral and vertical semipermeable drainage boundaries under time-dependent loading. *International Journal of Geomechanics*, *22*(12), 06022032. https://doi.org/10.1061/(ASCE)GM.1943-5622.0002508

[15] Shen, L., Qian, B., & Li, L. (2024). Axisymmetric consolidation behavior of multilayered unsaturated soils with transversely isotropic permeability. *Frontiers in Earth Science*, *12*, 1483314. https://doi.org/10.3389/feart.2024.1483314

[16] Li, L., Qin, A., Jiang, L., & Wang, L. (2023). Simplified mathematical modeling to plane strain consolidation considering unsaturated and saturated conditions for ground with anisotropic permeability. *Computers and Geotechnics*, *154*, 105150. https://doi.org/10.1016/j.compgeo.2022.105150

[17] Chen, G., Huang, Q., Gong, H., & Sun, Y. (2025). Modeling aquifer compaction and lateral deformation due to groundwater extraction: A comparative study using Terzaghi's and Biot's Theories. *Processes*, *13*(12), 4006. https://doi.org/10.3390/pr13124006

[18] Basack, S., & Nimbalkar, S. (2023). Load-settlement characteristics of stone column reinforced soft marine clay deposit: Combined field and numerical studies. *Sustainability*, *15*(9), 7457. https://doi.org/10.3390/SU15097457

[19] Theodore, A., Demir, A., & Yildiz, A. (2024). 2D numerical analysis of prefabricated vertical drains using different matching methods. *Applied Sciences*, *14*(12), 4970. https://doi.org/10.3390/app14124970

[20] Shuhaib, Z. K., & Khassa, S. I. (2024). Influence of permeability anisotropy on seepage and slope stability of an earthen dam during rapid and slow drawdown. *Mathematical Modelling of Engineering Problems*, *11*(5), 1355–1365. https://doi.org/10.18280/mmep.110527

[21] Xia, C., Lu, G., Bai, D., Zhu, Z., Luo, S., & Zhang, G. (2020). Sensitivity analyses of the seepage and stability of layered rock slope based on the anisotropy of hydraulic conductivity: A case study in the Pulang Region of Southwestern China. *Water*, *12*(8), 2314. https://doi.org/10.3390/w12082314

[22] Yeh, H. F., & Tsai, Y. J. (2018). Analyzing the effect of soil hydraulic conductivity anisotropy on slope stability using a coupled hydromechanical framework. *Water (Switzerland)*, *10*(7), 905. https://doi.org/10.3390/w10070905

[23] Zhao, L. H., Dai, P. G., Meng, Q. Y., Wang, W. M., Liu, S. F., & Ding, X. H. (2026). Analytical study of 2D consolidation in anisotropic soils under non-uniform loads and semi-permeable boundaries. *Physics and Chemistry of the Earth, Parts A/B/C*, *143*, 104310. https://doi.org/10.1016/j.pce.2026.104310

[24] Coduto, D. P., Kitch, W. A., & Yeung, M. C. R. (2022). *Foundation design: Principles and practices* (*3rd* ed.) . UK: Pearson.

[25] Das, B. M., & Sivakugan, N. (2018). *Principles of Foundation Engineering. Cengage Learning*. https://www.cengage.com/c/principles-of-foundation-engineering-9e-das-sivakugan/9781337705028/

[26] Dai, S., Jiang, L., Qin, A., & Liao, Y. (2025). Semi-Analytical solutions for one-dimensional consolidation of viscoelastic unsaturated soils considering variable permeability coefficient. *Applied Sciences*, *15*(9), 4918. https://doi.org/10.3390/app15094918

[27] Zienkiewicz, O. C., Taylor, R. L., & Zhu, J. Z. (2005). *The finite element method: Its basis and fundamentals*. UK: Elsevier Butterworth-Heinemann.

[28] Bentley Systems. (2025). *PLAXIS 2D Reference Manual*. https://files.seequent.com/PLAXIS/Manuals/PLAXIS_2D/English/PLAXIS_2D_2_Reference%20Manual.pdf

[29] Uysal, F., Bağrıaçık, B., & Yıldız, A. (2018). Yumuşak zemin model parametrelerinin zemin davranışına etkisi. *Çukurova Üniversitesi Mühendislik-Mimarlık Fakültesi Dergisi*, *33*(1), 97–106. https://doi.org/10.21605/cukurovaummfd.420681